

Unified multifractal description of longitudinal and transverse intermittency in fully developed turbulence

Dhawal Buaria^{1,*}

¹*Department of Mechanical Engineering, Texas Tech University, Lubbock, TX 79409*

(Dated: January 21, 2026)

Small-scale intermittency is a defining feature of fully developed fluid turbulence, marked by rare and extreme fluctuations of velocity increments and gradients that defy mean-field descriptions. Existing multifractal descriptions of intermittency focus primarily on longitudinal increments and gradients, despite mounting evidence that transverse components exhibit distinct and stronger intermittency. Here, we develop a unified multifractal framework that jointly prescribes longitudinal and transverse velocity increments, and extends to gradients. We derive explicit relations linking inertial-range scaling exponents of structure functions to moments of velocity gradients in dissipation range. Our results reveal that longitudinal gradient scaling is solely prescribed by longitudinal structure functions, as traditionally expected; however, transverse gradient scaling is prescribed by mixed longitudinal-transverse structure functions. Validation with high-resolution direct numerical simulations of isotropic turbulence, at Taylor-scale Reynolds number up to 1300 demonstrates excellent agreement, paving way for a more complete and predictive description of intermittency faithful to the underlying turbulence dynamics.

Intermittency, the spontaneous emergence of rare, intense fluctuations interspersed within otherwise quiescent dynamics, is a hallmark of complex far-from-equilibrium systems [1–4]. From a statistical standpoint, it is characterized by pronounced departures from Gaussianity emanating from a breakdown of simple self-similarity arguments, leading to anomalous scaling laws and dominance of extreme events in high-order moments [5, 6]. Fluid turbulence provides a paradigmatic example, where intermittency naturally manifests as energy is transferred from large to small scales, engendering rare and intense fluctuations of velocity increments and gradients at the small scales [1, 7]. These events, playing a crucial role in dissipation, mixing and transport, invalidate the mean-field description proposed in the seminal work of Kolmogorov (1941) [8], hereafter K41. Despite decades of progress, their quantitative characterization remains incomplete and a central obstacle to a universal description of small-scale turbulence [9].

The intermittency of velocity increments may be analyzed through its longitudinal component: $\delta u_r = u(x+r) - u(x)$, where the velocity component $u(x)$ is in the direction of the separation r ; or the transverse component; $\delta v_r = v(x+r) - v(x)$, corresponding to velocity component $v(x)$ orthogonal to separation direction. Building upon K41, one expects the moments of these increments, called structure functions, to exhibit anomalous power-law scalings in the inertial-range $\eta \ll r \ll L$, where L is the large scale and η is the viscous cutoff scale [1, 7]. At the smallest scales, these increments naturally lead to the longitudinal and transverse velocity gradients, $\partial_x u = \lim_{r \rightarrow 0} \delta u_r / r$ and $\partial_x v = \lim_{r \rightarrow 0} \delta v_r / r$, respectively, which directly relate to energy dissipation and enstrophy, and characterize intermittency at the viscous scales.

One can loosely equate the longitudinal and trans-

verse quantities to stretching and rotational motions of turbulent eddies, respectively, which are intimately coupled through the Navier-Stokes dynamics and are the key mechanisms driving the energy cascade [10–12]. Despite this duality, traditional descriptions of intermittency—most notably multifractal models [7, 13, 14]—have focused primarily on describing longitudinal velocity increments and gradients [15], with transverse statistics simply presumed to follow identical scaling relations as their longitudinal counterparts. However, this viewpoint has become untenable in light of substantial experimental and numerical evidence demonstrating disparate anomalous scaling behaviors between longitudinal and transverse statistics, with the latter being more intermittent [16–23]. These observations underscore the need for a unified framework capable of capturing both longitudinal and transverse statistics for an accurate and complete description of intermittency.

In this Letter, motivated by the above consideration, we develop a joint multifractal framework which simultaneously prescribes longitudinal and transverse velocity increments, and extend it to velocity gradients. We derive generalized relations directly relating the scaling exponents of structure functions in the inertial-range to those of gradient moments in the dissipation range. We find that the scaling of longitudinal gradients is solely prescribed by inertial-range exponents of longitudinal structure functions, consistent with traditional single-variable multifractal description. In contrast, the scaling of transverse gradients is governed not by transverse structure functions alone, but rather mixed longitudinal-transverse structure functions. These predictions are validated against high-resolution direct numerical simulations (DNS) of isotropic turbulence, showing remarkable agreement, and establishing a unified, predictive framework for intermittency that captures both longitudinal

and transverse statistics.

Joint multifractal framework: In traditional univariate multifractal description, the longitudinal velocity increment across a scale r is taken to be locally Hölder continuous: $\delta u_r \sim U(r/L)^h$, where the exponent h varies in the interval $[h_{\min}, h_{\max}]$. Here, U represents the large-scale velocity, typically given by the rms of velocity fluctuations. Each value of h is realized on a set with fractal dimension $D(h)$, also termed the multifractal spectrum, such that the probability to observe the exponent h at scale r is given as: $P_r(h) \sim (r/L)^{3-D(h)}$. Thereafter, one can appropriately obtain the scaling of structure functions and also gradient moments (see e.g. [7] for a detailed exposition). In principle, a similar description can be formulated for transverse increment δv_r [24], but with the drawback that it completely ignores any coupling between longitudinal and transverse components, which is known to play a central role in intermittency [11, 12, 20, 25–27].

The above shortcoming can be resolved by considering a bivariate multifractal description [28]. The essential idea is that we jointly consider longitudinal and transverse increments to be Hölder continuous

$$\delta u_r \sim U(r/L)^{h_1}, \quad \delta v_r \sim U(r/L)^{h_2}, \quad (1)$$

with exponents h_1 and h_2 prescribed by a joint multifractal spectrum $D(h_1, h_2)$ and the corresponding probability $P_r(h_1, h_2) \sim (r/L)^{3-D(h_1, h_2)}$. Thereafter, the mixed-structure functions of order p_1, p_2 in longitudinal and transverse directions can be obtained by integrating over the full bivariate distribution

$$\begin{aligned} & \langle (\delta u_r)^{p_1} (\delta v_r)^{p_2} \rangle / U^{p_1+p_2} \\ & \sim \int \int \left(\frac{r}{L} \right)^{p_1 h_1 + p_2 h_2 + 3 - D(h_1, h_2)} dh_1 dh_2. \end{aligned} \quad (2)$$

From the steepest descent estimation in the limit $r/L \rightarrow 0$, it follows that

$$\frac{\langle (\delta u_r)^{p_1} (\delta v_r)^{p_2} \rangle}{U^{p_1+p_2}} \sim \left(\frac{r}{L} \right)^{\zeta_{p_1, p_2}}, \quad (3)$$

with the scaling exponents given as

$$\zeta_{p_1, p_2} = \inf_{h_1, h_2} [p_1 h_1 + p_2 h_2 + 3 - D(h_1, h_2)]. \quad (4)$$

Thus, for a given value of p_1, p_2 , the critical Hölder exponents h_1^*, h_2^* which dictate the scaling exponents are obtained by solving the system:

$$\frac{\partial D}{\partial h_1}(h_1^*, h_2^*) = p_1, \quad \frac{\partial D}{\partial h_2}(h_1^*, h_2^*) = p_2. \quad (5)$$

We note that the work of [28] also considered similar joint multifractal measures, but for locally-averaged dissipation and enstrophy. Furthermore, it did not extend to gradients, which is performed next.

Extension to gradients: Combining the definitions of longitudinal and transverse gradients with Eq. (1) leads to

$$\partial_x u \sim \frac{U}{L} \left(\frac{r}{L} \right)^{h_1-1} \Big|_{r=\eta}, \quad \partial_x v \sim \frac{U}{L} \left(\frac{r}{L} \right)^{h_2-1} \Big|_{r=\eta}, \quad (6)$$

where η denotes the viscous cutoff scale. This scale is determined by imposing that the local Reynolds number of an eddy is unity [29, 30]. Conventionally, this condition is imposed using the longitudinal velocity increment:

$$\frac{\delta u_r}{\nu} = 1. \quad (7)$$

which combined with Eq. (1) and evaluated at $r = \eta$, gives

$$\eta/L \sim Re^{-1/(1+h_1)}. \quad (8)$$

where we have used $Re = UL/\nu$. It is easy to see that the Kolmogorov length scale $\eta_K = \eta(h_1 = \frac{1}{3})$. It is worth noting that the transverse increment, and in particular the exponent h_2 , does not play a role in determining η/L . This asymmetry is not coincidental, and we will return to it soon.

From Eq. (6), the joint moment of longitudinal and transverse gradients, of orders n_1 and n_2 , respectively, can be written as

$$\begin{aligned} & \frac{\langle (\partial_x u)^{n_1} (\partial_x v)^{n_2} \rangle}{(U/L)^{n_1+n_2}} \\ & \sim \int_h \left(\frac{r}{L} \right)^{n_1(h_1-1) + n_2(h_2-1) + 3 - D(h_1, h_2)} dh_1 dh_2 \Big|_{r=\eta}. \end{aligned} \quad (9)$$

Substituting the dissipative cutoff from Eq. 8 and invoking the steepest-descent argument in the limit $Re \rightarrow \infty$ yields the power-law dependence

$$\frac{\langle (\partial_x u)^{n_1} (\partial_x v)^{n_2} \rangle}{(U/L)^{n_1+n_2}} \sim Re^{\rho_{n_1, n_2}} \quad (10)$$

where the scaling exponent is given as

$$\rho_{n_1, n_2} = \sup_{h_1, h_2} \frac{n_1(1-h_1) + n_2(1-h_2) - 3 + D(h_1, h_2)}{1+h_1}. \quad (11)$$

The results in Eq. (4) and Eq. (11) constitute a natural generalization of the univariate multifractal model [7] to a joint description of longitudinal and transverse fluctuations. The knowledge of $D(h_1, h_2)$ uniquely determines the scaling exponents (of both structure functions and gradient moments). Conversely, the knowledge of any one set of exponents uniquely determines $D(h_1, h_2)$ through an appropriate Legendre transform, and thus fixes the other set as well. For instance, the

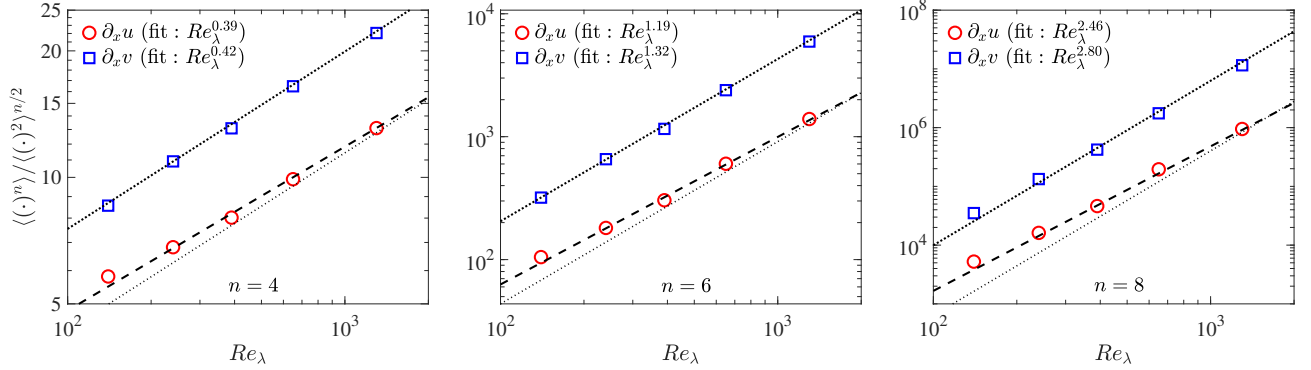


FIG. 1. Central moments of longitudinal and transverse velocity gradients for moment orders (a) 4, (b) 6, and (c) 8, together with the best-fit power-law scalings.

relation in Eq. (4) can be inverted to write: $D(h_1, h_2) = \inf_{p_1, p_2} [p_1 h_1 + p_2 h_2 + 3 - \zeta_{p_1, p_2}]$.

To that end, the mixed-gradient exponents ρ_{n_1, n_2} can be directly related to mixed-increment exponents ζ_{p_1, p_2} without explicitly using $D(h_1, h_2)$. As shown in the Appendix B, this yields the result

$$\rho_{n_1, n_2} = p_1(n_1, n_2) - n_1. \quad (12)$$

where the function $p_1(n_1, n_2)$ is obtained as the solution of

$$\zeta_{p_1, p_2} + (p_1 + p_2) = 2(n_1 + n_2), \quad (13)$$

$$p_2 = n_2. \quad (14)$$

This provides a generalized result relating the scaling of velocity gradients to that of increments in the inertial-range. Defining

$$p_1 + p_2 = p, \quad n_1 + n_2 = n, \quad (15)$$

we can more compactly write $\rho_{n_1, n_2} = p - n$, with p being the solution of

$$\zeta_{p-n_2, n_2} + p = 2(n_1 + n_2). \quad (16)$$

Longitudinal and transverse gradients: Consider now the two cases 1) $n_2 = 0$ (and $n_1 = n$), and 2) $n_1 = 0$ (and $n_2 = n$), which isolate the scaling of longitudinal and transverse gradients, respectively. For these cases, Eq. (16) yields

$$\zeta_{p, 0} + p = 2n, \quad (n_2 = 0, n_1 = n), \quad (17)$$

$$\zeta_{p, n} + p = 2n, \quad (n_1 = 0, n_2 = n). \quad (18)$$

The first relation in Eq. (17) implies that the exponents for longitudinal gradients $\rho_{n, 0}$ are prescribed solely by longitudinal scaling exponents $\zeta_{p, 0}$. In fact, this result is identical to that obtained from conventional univariate multifractal description of longitudinal statistics [7, 31]. In striking contrast, Eq. (18) reveals that the exponents

for transverse gradients $\rho_{0, n}$ are determined *not* by transverse structure functions $\zeta_{0, p}$, but rather by mixed exponents $\zeta_{p-n, n}$.

It is worth emphasizing that this inherent asymmetry in scaling of longitudinal and transverse gradients is rooted in how the dissipative cutoff η/L is defined (in Eq. (8)) solely from the longitudinal increment. If the cutoff was instead defined from the transverse increment, one would obtain the result that scaling of longitudinal gradients is tied to scaling of mixed-structure functions, while the transverse statistics are self-prescribed. Alternatively, if the dissipative cutoff was defined from a combination of increments [32], then both longitudinal and transverse gradients would be tied mixed structure function exponents. However, such considerations can easily be ruled out by appealing to known results imposed by dissipation anomaly.

For the case $(n_1, n_2) = (2, 0)$, i.e., scaling of $\langle(\partial_x u)^2\rangle$, Eq. (17) is satisfied for $p = 3$, $\zeta_{3, 0} = 1$, leading to $\rho_{2, 0} = 1$, which correspond to the well-known 4/5-th law, $\langle(\delta u_r)^3\rangle = -\frac{4}{5}\langle\epsilon\rangle r$ and dissipation anomaly, $\nu\langle(\partial_x u)^2\rangle \sim 1$. Likewise, for $(n_1, n_2) = (0, 2)$, i.e., scaling of $\langle(\partial_x v)^2\rangle$, Eq. (18) is satisfied for $p = 3$, $\zeta_{1, 2} = 1$, also leading to $\rho_{0, 2} = 1$, which correspond to the 4/3-th law, $\langle\delta u_r(\delta v_r)^2\rangle = -\frac{4}{3}\langle\epsilon\rangle r$ and dissipation anomaly. In fact, the results $\zeta_{3, 0} = \zeta_{1, 2} = 1$ are already well-known to be the only exactly derivable results from Navier-Stokes equations, reflecting a fundamental asymmetry between longitudinal and transverse statistics [33]. The relations in Eqs. (17)-(18) show how this asymmetry propagates to the scaling of velocity gradients and generalizes it to higher orders within the joint multifractal framework.

Validation with DNS results: To assess the validity of the proposed framework, we next test the predictions in Eqs. (17)-(18) with results from DNS. The DNS database utilized is identical to that in several recent works [25, 27, 34–37] and is briefly described in Appendix A. Before analyzing the scalings, a couple of important considerations should be noted. The inertial-range exponents for structure functions are expected to be indepen-

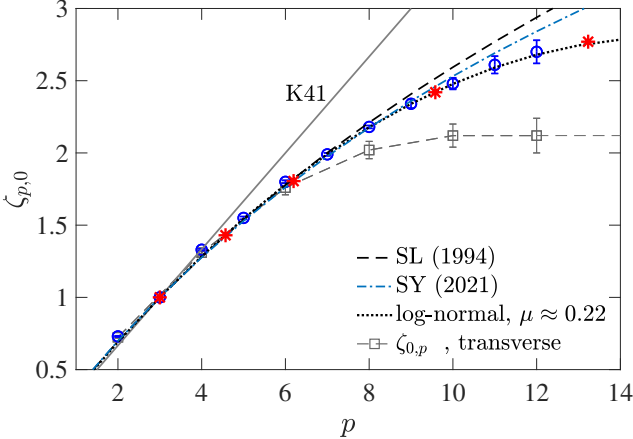


FIG. 2. Longitudinal inertial-range scaling exponents $\zeta_{p,0}$ versus p . Integer-order exponents (blue circles) are obtained directly from structure functions and were reported previously [21, 22], while non-integer orders (red asterisks) are inferred from velocity gradient moments using Eq. (21), for $n = 2, 3, 4, 6, 8$. For reference, theoretical predictions [14, 30, 40] and the transverse exponents $\zeta_{0,p}$ are also shown.

dent of Re , with only the extent of power-laws increasing with Re . In contrast, the scaling of gradient moments explicitly depends on Re , and care must be taken to accurately extract the exponents at high Re . In some recent studies [23, 30], it was argued that asymptotic power-law scalings for gradient moments already manifest at low Re . Compiling data from various sources with that of our own at higher Re , we show in Appendix C that this is not actually the case, and asymptotic power-laws for gradient moments also only arise at high Re .

Retaining only the DNS at high enough Re_λ , the scaling of longitudinal and transverse gradient moments is shown in Fig. 1. The central moments as a function of Re_λ are shown, highlighting small but clear differences between scaling of longitudinal and transverse moments. The expression in Eq. (10) can be modified for central moments defined as

$$M_{n_1, n_2} \equiv \frac{\langle (\partial_x u)^{n_1} (\partial_x v)^{n_2} \rangle}{\langle (\partial_x u)^2 \rangle^{n_1/2} \langle (\partial_x v)^2 \rangle^{n_2/2}} \sim Re_\lambda^{\xi_{n_1, n_2}} \quad (19)$$

$$\text{with , } \xi_{n_1, n_2} = 2\rho_{n_1, n_2} - n_1 - n_2 = 2p - 3n \quad (20)$$

where we have used $Re \sim Re_\lambda^2$ and $\rho_{2,0} = \rho_{0,2} = 1$. It is easy to see that $\xi_{2,0} = \xi_{0,2} = 0$, whereas the results in Fig. 1 provide $\xi_{n,0}$ and $\xi_{0,n}$ for $n = 4, 6, 8$. Additionally, the result for skewness of longitudinal gradients, $\xi_{3,0} \approx 0.14$ is adopted from earlier works [25, 38, 39].

Focusing first on longitudinal statistics, to validate the result in Eq. (17), we simply invert the relation $\xi_{n,0} = 2p - 3n$ and Eq. (17) to solve for p and $\zeta_{p,0}$, leading

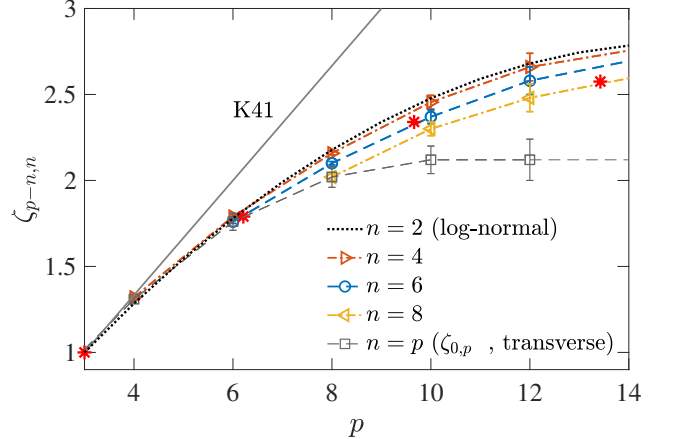


FIG. 3. Mixed inertial-range scaling exponents $\zeta_{p-n,n}$ versus p for various integer values of n (see legend). Exponents at integer p are obtained directly from structure functions, while non-integer orders (red asterisks) are inferred from the scaling of transverse velocity gradient moments using Eq. (22) for $n = 2, 4, 6, 8$. The dashed curve for $n = 2$ corresponds to the log-normal prediction from Fig. 2 and represents $\zeta_{p-2,2}$ (which is identical to $\zeta_{p,0}$ [30]).

to

$$p = (3n + \xi_{n,0})/2 , \quad \zeta_{p,0} = 2n - p . \quad (21)$$

It is easy to see that these relations imply $3n/2 < p < 2n$, suggesting that n -th order gradient arise from structure functions of order greater than $3n/2$ but smaller than $2n$. Now for various n and $\xi_{n,0}$ from Fig. 1, we can obtain pairs of p and $\zeta_{p,0}$, and compare them with known results for longitudinal inertial-range exponents directly obtained from structure functions. This comparison is shown in Fig. 2, with exponents for integer p values obtained from recent works [21, 22]. and non-integer p values corresponding to scaling exponents of longitudinal gradients for $n = 2, 3, 4, 6, 8$. Evidently, remarkable agreement is obtained between them, with all exponents near-perfectly described by the log-normal prediction (with intermittency exponent $\mu \approx 0.22$ [41].)

Is it well-known that the log-normal prediction is untenable for large p values [7], nevertheless, it serves as a remarkable approximation of the exponents up to orders shown in Fig. 2. For comparison, we also show the theoretical predictions of [14, 30], which show conspicuous deviations for large p . For this reason, any predictions for gradient exponents even at modest orders obtained from these results would deviate from DNS results, as was the case in [42]. While a fully accurate theoretical prediction for $\zeta_{p,0}$ for highest orders remains elusive, it is evident from Fig. 2, that scaling of structure functions and gradient moments as described by the joint multi-fractal framework is fully self-consistent.

Next, focusing on transverse gradients, we can invert

$\xi_{0,n} = 2p - 3n$ and Eq. (18) to write

$$p = (3n + \xi_{0,n})/2, \quad \zeta_{p-n,n} = 2n - p. \quad (22)$$

Thus, in this case, each gradient moment of order n , falls on a different branch of mixed structure function prescribed by $\zeta_{p-n,n}$. To that end, we evaluate these exponents for $n = 2, 4, 6, 8$ from $\xi_{0,n}$, and simultaneously extract $\zeta_{p-n,n}$ directly from mixed structure functions in the inertial-range (the latter by extending the procedures in [21, 22]). These results are shown in Fig. 3. Incidentally, we find that $\zeta_{p-2,2} \approx \zeta_{p,0}$, for $p \geq 2$, which has been theoretically suggested before [30]. Remarkably, we observe that the results for $p, \zeta_{p-n,n}$ obtained from gradient exponents fall near perfectly on different branches of $\zeta_{p-n,n}$ obtained from structure functions for integer values of p .

Conclusions: To summarize, we have developed here a unified multifractal framework that jointly describes longitudinal and transverse intermittency in fully developed turbulence, naturally linking intermittency of velocity increments in the inertial-range and that of gradients at the dissipative scales. Our analysis reaffirms that longitudinal gradient statistics are prescribed solely by longitudinal structure functions, however, transverse gradient statistics are governed by mixed structure functions. The resulting predictions show near-perfect agreement with DNS data, establishing both the consistency and accuracy of the framework.

Our results clearly emphasize that a complete and faithful description of intermittency requires simultaneous consideration of longitudinal and transverse fluctuations, and hence intrinsically coupled dynamics of stretching and rotational motions encoded in Navier-Stokes equations. While recent studies have also hinted at this [12, 20, 26, 37, 43], the present work now provides an explicit statistical framework for it. Although the framework establishes precise connections between inertial and dissipation-range statistics, it does not yet furnish a closed description for the full set of mixed exponents ζ_{p_1,p_2} , which remains an outstanding challenge. Addressing this gap will surely require development of intermittency models that embrace the tensorial nature of underlying turbulence dynamics.

The unified description developed here also carries potential implications for turbulence modeling. By explicitly accounting for the coupled nature of longitudinal and transverse intermittency, it offers a natural pathway towards improved representation of small-scales in reduced-order models and large-eddy simulations. Additionally, the framework also opens several promising directions for future investigation, including extensions to Lagrangian intermittency—especially acceleration statistics, which have proven particularly challenging to characterize under the multifractal framework [39, 44]. Progress along these directions will be reported as future work.

Acknowledgments: We gratefully acknowledge the Gauss Centre for Supercomputing e.V. (www.gauss-center.eu) for providing time on the supercomputers JUQUEEN and JUWELS at Jülich Supercomputing Centre (JSC), where the simulations reported in this paper were performed. We are also grateful to Sualeh Khurshid and Toshiyuki Gotoh for sharing the data points used in Fig. 4.

* dhawal.buaria@ttu.edu

- [1] K. R. Sreenivasan and R. A. Antonia, The phenomenology of small-scale turbulence, *Annu. Rev. Fluid Mech.* **29**, 435 (1997).
- [2] R. Bruno and V. Carbone, The solar wind as a turbulence laboratory, *Living Rev. Sol. Phys.* **10**, 2 (2013).
- [3] W. H. Matthaeus, M. Wan, S. Servidio, A. Greco, K. T. Osman, S. Oughton, and P. Dmitruk, Intermittency, nonlinear dynamics and dissipation in the solar wind and astrophysical plasmas, *Phil. Trans. R. Soc. A* **373**, 20140154 (2015).
- [4] S. N. Majumdar, A. Pal, and G. Schehr, Extreme value statistics of correlated random variables: a pedagogical review, *Phys. Rep.* **840**, 1 (2020).
- [5] B. I. Halperin and P. C. Hohenberg, Scaling laws for dynamic critical phenomena, *Phys. Rev.* **177**, 952 (1969).
- [6] G. Paladin and A. Vulpiani, Anomalous scaling laws in multifractal objects, *Phys. Rep.* **156**, 147 (1987).
- [7] U. Frisch, *Turbulence: the legacy of Kolmogorov* (Cambridge University Press, Cambridge, 1995).
- [8] A. N. Kolmogorov, The local structure of turbulence in an incompressible fluid for very large Reynolds numbers, *Dokl. Akad. Nauk. SSSR* **30**, 9 (1941).
- [9] K. R. Sreenivasan and J. Schumacher, What is the turbulence problem, and when may we regard it as solved?, *Annu. Rev. Condens. Matter Phys.* **16**, 121 (2025).
- [10] A. Tsinober, *An Informal Conceptual Introduction to Turbulence* (Springer, Berlin, 2009).
- [11] M. Carbone and A. D. Bragg, Is vortex stretching the main cause of the turbulent energy cascade?, *J. Fluid Mech.* **883**, R2 (2020).
- [12] P. L. Johnson, Energy transfer from large to small scales in turbulence by multi-scale nonlinear strain and vorticity interactions, *Phys. Rev. Lett.* **124**, 104501 (2020).
- [13] C. Meneveau and K. R. Sreenivasan, The multifractal nature of turbulent energy dissipation, *J. Fluid Mech.* **224**, 429– (1991).
- [14] Z.-S. She and E. Leveque, Universal scaling laws in fully developed turbulence, *Phys. Rev. Lett.* **72**, 336 (1994).
- [15] A reason for this is that only the 1D longitudinal component along the streamwise direction was accessible in early wind tunnel experiments. Also, it is arguably easier to pose turbulence theory in terms of longitudinal increments, since the the 4/5-th law, corresponding to its third moment, is exactly derivable from Navier-Stokes equations. In contrast, the 4/3-th law is also exactly derivable, but requires both longitudinal and transverse increments [7].
- [16] B. Dhruva, Y. Tsuji, and K. R. Sreenivasan, Transverse structure functions in high-reynolds-number turbulence,

Phys. Rev. E **56**, R4928 (1997).

[17] S. Chen, K. R. Sreenivasan, M. Nelkin, and N. Cao, Refined similarity hypothesis for transverse structure functions in fluid turbulence, Phys. Rev. Lett. **79**, 2253 (1997).

[18] X. Shen and Z. Warhaft, Longitudinal and transverse structure functions in sheared and unsheared wind-tunnel turbulence, Phys. Fluids **14**, 370 (2002).

[19] B. Dubrulle, Beyond Kolmogorov cascades, J. Fluid Mech. **12** (2019).

[20] D. Buarria, A. Pumir, E. Bodenschatz, and P. K. Yeung, Extreme velocity gradients in turbulent flows, New J. Phys. **21**, 043004 (2019).

[21] K. P. Iyer, K. R. Sreenivasan, and P. K. Yeung, Scaling exponents saturate in three-dimensional isotropic turbulence, Phys. Rev. Fluids **5**, 054605 (2020).

[22] D. Buarria and K. R. Sreenivasan, Saturation and multifractality of lagrangian and eulerian scaling exponents in three-dimensional turbulence, Phys. Rev. Lett. **131**, 204001 (2023).

[23] S. Khurshid, D. A. Donzis, and K. R. Sreenivasan, Emergence of universal scaling in isotropic turbulence, Phys. Rev. E **107**, 045102 (2023).

[24] One can consider a different and independent multifractal spectrum compared to the longitudinal counterpart, or can also assume they are the same.

[25] D. Buarria, E. Bodenschatz, and A. Pumir, Vortex stretching and enstrophy production in high Reynolds number turbulence, Phys. Rev. Fluids **5**, 104602 (2020).

[26] D. Buarria and A. Pumir, Vorticity-strain rate dynamics and the smallest scales of turbulence, Phys. Rev. Lett. **128**, 094501 (2022).

[27] D. Buarria, A. Pumir, and E. Bodenschatz, Generation of intense dissipation in high Reynolds number turbulence, Philos. Trans. R. Soc. A **380**, 20210088 (2022).

[28] C. Meneveau, K. R. Sreenivasan, P. Kailasnath, and M. S. Fan, Joint multifractal measures: Theory and applications to turbulence, Phys. Rev. A **41**, 894 (1990).

[29] G. Paladin and A. Vulpiani, Degrees of freedom of turbulence, Phys. Rev. A **35**, 1971 (1987).

[30] K. R. Sreenivasan and V. Yakhot, Dynamics of three-dimensional turbulence from navier-stokes equations, Phys. Rev. Fluids **6**, 104604 (2021).

[31] M. Nelkin, Multifractal scaling of velocity derivatives in turbulence, Phys. Rev. A **42**, 7226 (1990).

[32] For instance, this can be done by defining the cutoff scale using the condition: $(\delta u_r)^\alpha (\delta v_r)^{1-\alpha} r/\nu \simeq 1$, where $0 < \alpha < 1$ is some parameter that needs to be determined.

[33] Note that from simple symmetry arguments, it is easy to deduce that $\zeta_{0,3} = 0$.

[34] D. Buarria, A. Pumir, and E. Bodenschatz, Self-attenuation of extreme events in Navier-Stokes turbulence, Nat. Commun. **11**, 5852 (2020).

[35] D. Buarria and K. R. Sreenivasan, Dissipation range of the energy spectrum in high Reynolds number turbulence, Phys. Rev. Fluids **5**, 092601(R) (2020).

[36] D. Buarria and A. Pumir, Nonlocal amplification of intense vorticity in turbulent flows, Phys. Rev. Research **3**, 042020 (2021).

[37] D. Buarria and A. Pumir, Role of pressure in the dynamics of intense velocity gradients in turbulent flows, J. Fluid Mech. **973**, A23 (2023).

[38] T. Ishihara, Y. Kaneda, M. Yokokawa, K. Itakura, and A. Uno, Small-scale statistics in high resolution of numerically isotropic turbulence, J. Fluid Mech. **592**, 335 (2007).

[39] D. Buarria and K. R. Sreenivasan, Lagrangian acceleration and its Eulerian decompositions in fully developed turbulence, Phys. Rev. Fluids **8**, L032601 (2023).

[40] A. N. Kolmogorov, A refinement of previous hypotheses concerning the local structure of turbulence in a viscous incompressible fluid at high Reynolds number, J. Fluid Mech. **13**, 82 (1962).

[41] D. Buarria and K. R. Sreenivasan, Intermittency of turbulent velocity and scalar fields using three-dimensional local averaging, Phys. Rev. Fluids **7**, L072601 (2022).

[42] G. E. Elsinga, T. Ishihara, and J. C. R. Hunt, Intermittency across reynolds numbers—the influence of large-scale shear layers on the scaling of the enstrophy and dissipation in homogenous isotropic turbulence, J. Fluid Mech. **974**, A17 (2023).

[43] M. Carbone, M. Iovieno, and A. D. Bragg, Symmetry transformation and dimensionality reduction of the anisotropic pressure hessian, J. Fluid Mech. **900**, A38 (2020).

[44] D. Buarria and K. R. Sreenivasan, Scaling of acceleration statistics in high Reynolds number turbulence, Phys. Rev. Lett. **128**, 234502 (2022).

[45] G. S. Patterson and S. A. Orszag, Spectral calculations of isotropic turbulence: efficient removal of aliasing interactions, Phys. Fluids **14**, 2538 (1971).

[46] R. S. Rogallo, Numerical experiments in homogeneous turbulence, NASA Technical Memo (1981).

[47] V. Eswaran and S. B. Pope, An examination of forcing in direct numerical simulations of turbulence, Comput. Fluids **16**, 257 (1988).

[48] D. Buarria, J. M. Lawson, and M. Wilczek, Twisting vortex lines regularize Navier-Stokes turbulence, Science Advances **10** (2024).

[49] D. Buarria and A. Pumir, Universality of extreme events in turbulent flows, Phys. Rev. Fluids **10**, L042601 (2025).

[50] T. Gotoh and J. Yang, Transition of fluctuations from gaussian state to turbulent state, Philos. Trans. R. Soc. A **380**, 20210097 (2022).

[51] R. Benzi, S. Ciliberto, R. Tripiccione, C. Baudet, F. Massaioli, and S. Succi, Extended self-similarity in turbulent flows, Phys. Rev. E **48**, R29 (1993).

[52] J. Schumacher, J. D. Scheel, D. Krasnov, D. A. Donzis, V. Yakhot, and K. S. Sreenivasan, Small-scale universality in fluid turbulence, Proc. Natl. Acad. Sci. **111**, 10961 (2014).

Appendix A – DNS data

The DNS data utilized here are obtained by solving the incompressible Navier-Stokes equations:

$$\partial \mathbf{u} / \partial t + (\mathbf{u} \cdot \nabla) \mathbf{u} = -\nabla P + \nu \nabla^2 \mathbf{u} + \mathbf{f}, \quad (23)$$

where \mathbf{u} is the divergence-free velocity ($\nabla \cdot \mathbf{u} = 0$), P is the kinematic pressure, and \mathbf{f} is the forcing term. The simulations correspond to the canonical setup of forced isotropic turbulence in a cubic domain with periodic boundary conditions. This allows us to use highly accurate Fourier pseudo-spectral methods, with aliasing error controlled by a combination of truncation and phase-shifting [45, 46]. The largest scales are forced stochastically to maintain a statistically stationary state [47]. The domain size is $(2\pi)^3$, discretized into N^3 grid points, with uniform grid-spacing $\Delta x = 2\pi/N$ in each direction. The Taylor-scale Reynolds number Re_λ goes from 140 to 1300 – on grid sizes 1024^3 to 12288^3 , respectively, thus maintaining excellent small scale resolution [20, 25]. As mentioned earlier, the precise data have been used in numerous recent studies [25, 27, 34–37], which have adequately established convergence with respect to resolution and statistical sampling. In fact, in some recent studies [48, 49], detailed comparisons have also been made with laboratory experiments and DNS of some anisotropic flows, showing excellent quantitative agreement.

Appendix B – Derivation of Eqs. (12)–(14)

For the result in Eq. (11), defining the critical Hölder exponents as h_1^* and h_2^* , the right-hand side yields the following after taking the derivatives

$$(1 + h_1^*)(-n_1 + \partial D / \partial h_1) - [n_1(1 - h_1^*) + n_2(1 - h_2^*) - 3 + D] = 0, \quad (24)$$

$$-n_2 + \partial D / \partial h_2 = 0. \quad (25)$$

Substituting $\partial D / \partial h_1 = p_1$, $\partial D / \partial h_2 = p_2$ from Eq. (5) and $-3 + D = p_1 h_1^* + p_2 h_2^* - \zeta_{p_1, p_2}$ from Eq. (4) then yields

$$\zeta_{p_1, p_2} + p_1 = 2n_1 + n_2 + (p_2 - n_2)h_2^*, \quad (26)$$

$$p_2 = n_2, \quad (27)$$

which can be readily simplified to give the results in Eqs. (13)–(14). The result in Eq. (12) can be obtained by combining the result in Eq. (24) with that in Eq. (11).

Appendix C – Asymptotic scaling of gradient moments

Recently, there has been some debate as to when precisely does the asymptotic scaling of velocity gradient

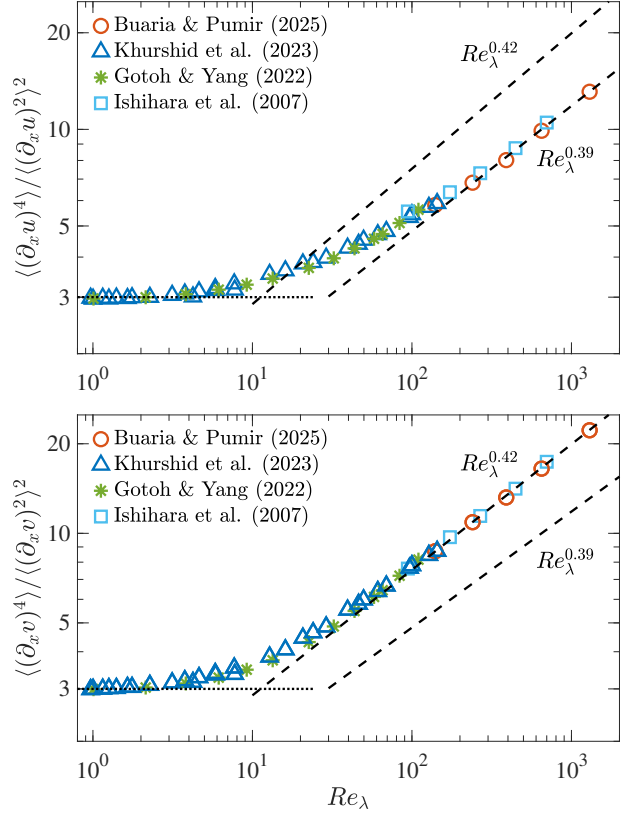


FIG. 4. Flatness of longitudinal (top) and transverse (bottom) velocity gradients, compiled using data from various sources [23, 38, 49, 50]. The best-fit power-law scaling are also marked in dashed lines. The dotted horizontal line at 3 marks the flatness of a standard Gaussian distribution.

moments emerges as a function of Re_λ . When considering inertial-range scaling of structure functions, the scaling exponents emerge as plateaus on local slope plots, with only the extent of the plateau increasing with Re_λ , but the value itself being independent of Re_λ . See e.g. [21, 22] for results at the Re_λ considered in this work. The use of extended self-similarity [51] can often provide a more robust plateau, especially at lower Re_λ . In contrast, the situation for gradient moments is tricky, since the scaling exponents have to be directly extracted as a function of Re_λ . Classical theoretical arguments dictate that scaling exponents for gradients should also require high Re_λ . However, some recent studies [23, 30, 52] have suggested that asymptotic scaling of gradient moments emerges at very low Re_λ ($\gtrsim 10$), substantially lower than dictated by theory. However, these studies were all restricted to $Re_\lambda \lesssim 200$, and therefore did not verify if the same scaling behaviors extend to much higher Re_λ , as considered here.

To resolve this, we have compiled data from DNS of isotropic turbulence from numerous sources [23, 38, 50] along with our own [49]. Figure 4 shows the flatness of longitudinal and transverse velocity gradients, spanning

three orders of magnitude in Re_λ (and six in Re), providing a comprehensive view of the scaling behavior. Excellent correspondence is obtained between all the data. Several important observations can be made from these plots. At very low Re_λ , the flatness starts at 3, which corresponds to a Gaussian distribution. With increasing Re_λ , the flatness steadily increases and approaches a clear asymptotic power-law only at the highest Re_λ (which are very slightly different for longitudinal and transverse gradients). The intermediate range, in particular $10 \lesssim Re_\lambda \lesssim 200$ clearly corresponds to some kind of smooth transition regime, where turbulence has not fully developed yet. Thus, any power-laws extracted in this regime, do not truly correspond to asymptotic scalings of gradient moments – contrary to what was proposed in earlier works [23, 30, 52]. Although not shown, same conclusions can also be drawn from the behavior of higher-order moments.

Interestingly, the work of [30], SY2021 henceforth, also provides a way to extract scaling of gradient moments from inertial range exponents. However, unlike the multifractal results derived in this work, their theory posits that gradient moments of order n directly result from structure functions of order $p = 2n$. The corresponding result in multifractal model gives $3n/2 < p < 2n$, resulting in stronger scaling laws than predicted by SY2021. In SY2021, the power-laws for gradient moments were ex-

tracted at low Re_λ , resulting in fortuitous agreement between the predictions from their theory. However, given the data at much higher Re_λ and the present theoretical developments, it stands to reason that the multifractal extension of inertial-range intermittency to gradients provides the correct result.

On a related note, the recent work of [42] has suggested that the true asymptotic scalings of gradients might still not have been realized, with exponents still increasing with Re_λ , and longitudinal and transverse exponents potentially becoming identical at extremely high Re_λ . This certainly cannot be ruled out given the highest Re_λ in DNS are still modest compared to what can be realized in geophysical flows. However, the trends in Fig. 4 definitely suggest any further change to the exponents, if happening, would be extremely slow. In fact, a simple extrapolation of current data trends would show that such a change might only become perceptible at $Re_\lambda \gtrsim 10,000$ (or even higher), well beyond what can be realized in DNS or laboratory experiments for the foreseeable future. Moreover, any change in scaling of gradients would also be accompanied by change in inertial-range exponents. These aspects certainly need to be kept in mind for future, but given the available data, the proposed joint multifractal framework appears to be self-consistent and accurate in explaining the scaling of longitudinal and transverse gradients.